Supplemental Material

Details on the short-term plasticity model (STP)

Short-term plasticity is a non-linear synaptic mechanism observed in cortical pyramidal neurons [1, 2, 3, 4]. In these synapses, the synaptic strength, measured as the amplitude of the postsynaptic potential, depends on the availability of presynaptic vesicles and their release probability [2]. Tsodysks and Markram [2] first proposed a model of short-term plasticity, which was later modified by Mongillo et al. [5], who introduced synaptic state binary variables. Here, we briefly summarize this STP model in spiking networks. For more detailed information, we refer to Ref. [5]. We then provide details on the approximation we have used in this study to derive the mean-field steady-state synaptic factor w^o.

Mongillo et al. [5] define STP variables x and y. At an individual synapse, x represents the availability of neurotransmitter and y is the binding state of calcium ions. Neurotransmitter can be available ($x = 1$) or not ($x = 0$) and calcium can be either bound ($y = 1$) or not ($y = 0$). If the presynaptic neuron spikes, calcium binds to the postsynaptic receptor with probability U. If calcium binds ($y = 1$) and neurotransmitter is available ($x = 1$), neurotransmitter is released ($x \to 1$) and the postsynaptic neuron spikes. In between spikes, neurotransmitter replenishes with rate $1/\tau_D$ ($x \to 1$) and calcium unbinds with rate $1/\tau_F$ ($y \to 0$). In a network context, Mongillo et al. [5] define

$$\begin{aligned}
\langle y\rangle_{k+1} &= [U + (1-U)\langle y\rangle_k]e^{\frac{-\Delta_{k+1}}{\tau_F}} \\
\langle x\rangle_{k+1} &= 1 - [1 - (1-U)(\langle x\rangle_k - \langle xy\rangle_k)]e^{\frac{-\Delta_{k+1}}{\tau_D}} \\
\langle xy\rangle_{k+1} &= (1 - e^{\frac{-\Delta_{k+1}}{\tau_D}})[U + (1-U)(\langle y\rangle_k]e^{\frac{-\Delta_{k+1}}{\tau_F}},
\end{aligned} \tag{S1}$$

where $\langle y\rangle$ denotes the fraction of synapses with calcium being available, $\langle x\rangle$ the fraction of synapses with neurotransmitter being available, and $\langle xy\rangle$ the fraction of synapses where both calcium and neurotransmitter are available. The probability of neurotransmitter release upon the $(k+1)$-th spike is $w_{k+1} = U\langle x\rangle_{k+1} + (1-U)\langle xy\rangle_{k+1}$. Mongillo et al. [5] compute the steady-state synaptic state as a function of the Laplace transform of the interspike interval probability distribution function. For arbitrary stationary interspike interval probability distribution functions, they derive the following steady-state values

$$\begin{aligned}
\langle y\rangle &= \frac{U\tilde{p}(\frac{1}{\tau_F})}{1-(1-U)\tilde{p}(\frac{1}{\tau_F})} \\
\langle x\rangle &= \frac{1-[1+(1-U)\langle xy\rangle]\tilde{p}(\frac{1}{\tau_D})}{1-(1-U)\tilde{p}(\frac{1}{\tau_D})} \\
\langle xy\rangle &= \left(1 - \frac{\tilde{p}(\frac{1}{\tau_D}+\frac{1}{\tau_F})}{\tilde{p}(\frac{1}{\tau_F})}\right)\langle y\rangle \\
w &= U\langle x\rangle + (1-U)\langle xy\rangle,
\end{aligned} \tag{S2}$$

where $\tilde{p}(s)$ is the Laplace transform of the interspike interval probability distribution function and w is the steady-state neurotransmitter release probability upon spike.

At this point, we assume an exponential interspike interval distribution function, which is characteristic of a Poisson process [6], to get the steady state mean-field approximation for w. In this case, the Laplace transform is $\tilde{p}(s) = \frac{\nu_E}{s+\nu_E}$, where ν_E is the presynaptic excitatory firing rate. Inserting this expression into Equations (S2) gives the following approximations for the synaptic steady-states $\langle y \rangle_{\nu_E}$, $\langle x \rangle_{\nu_E}$, $\langle xy \rangle_{\nu_E}$ and $w^o(\nu_E)$:

$$\begin{aligned}
\langle y \rangle_{\nu_E} &= \frac{U\nu_E}{U\nu_E + \frac{1}{\tau_F}} \\
\langle x \rangle_{\nu_E} &= \frac{1}{\tau_D} \frac{U^2\nu_E^2 + \frac{U\nu_E}{\tau_F} + \frac{1}{\tau_F^2} + \frac{U\nu_E}{\tau_D} + \frac{1}{\tau_D}\frac{1}{\tau_F}}{(\nu_E + \frac{1}{\tau_F} + \frac{1}{\tau_D})(U\nu_E + \frac{1}{\tau_D})} \\
\langle xy \rangle_{\nu_E} &= \frac{1}{\tau_D} \frac{U\nu_E}{(\nu_E + \frac{1}{\tau_F} + \frac{1}{\tau_D})(U\nu_E + \frac{1}{\tau_F})} \\
w^o(\nu_E) &= \frac{1}{\tau_D} \frac{U(\nu_E + \frac{1}{\tau_F})(U\nu_E + \frac{1}{\tau_F} + \frac{1}{\tau_D})}{(\nu_E + \frac{1}{\tau_F} + \frac{1}{\tau_D})(U\nu_E + \frac{1}{\tau_D})(U\nu_E + \frac{1}{\tau_F})}.
\end{aligned} \tag{S3}$$

$w^o(\nu_E)$ is the steady-state probability of neurotransmitter release as a function of the presynaptic excitatory firing rate ν_E and the synaptic parameters τ_F, τ_D and U (Figure S3). $w^o(\nu_E)$ is used in the mean-field description of networks with $E \to E$ STP (Models II, IV, and VI; Equation 5).

The susceptibility δ in networks with $E \to E$ and $E \to I$ plastic synapses.

Here, we expand the definition of δ in networks with $E \to E$ plasticity (Equation 2) to networks in which $E \to E$ and $E \to I$ synapses are plastic. We examine if the different types of contrast response described in Figure 2 for networks with $E \to E$ plasticity change through the introduction of $E \to E$ and $E \to I$ plastic synapses. To that end, we derive the stimulus contrast that drives a network to fire at rates ν_E and ν_I from Equation 10:

$$c(\nu_E, \nu_I) = \nu_E q p_E \frac{J_{EI}J_{IE}w^o_{IE}(\nu_E) - J_{EE}w^o_{EE}(\nu_E)J_{II}}{J_{II} - J_{EI}}, \tag{S4}$$

where we have set $w^o_{EI} = w^o_{II} = 1$ and $\mathrm{k}_{EI} = \mathrm{k}_{II} = 0$. Using the definition of k_{EE} (Equation 4), the derivative of the input contrast c with respect to the excitatory firing rate ν_E is inserted into Equation 1 to obtain

$$\delta = \frac{J_{EE}J_{II}w^o_{EE} - J_{EI}J_{IE}w^o_{IE}}{J_{EE}J_{II}w^o_{EE}(1+k_{EE}) - J_{EI}J_{IE}w^o_{IE}(1+k_{IE})}. \tag{S5}$$

We substitute $\beta = \frac{J_{EI}J_{IE}}{J_{II}J_{EE}}$, which yields

$$\delta = \frac{w^o_{EE} - \beta w^o_{IE}}{w^o_{EE}(1+k_{EE}) - \beta w^o_{IE}(1+k_{IE})}. \tag{S6}$$

We examine the non-linear contrast response of balanced networks with additional plastic $E \to I$ synapses for w_{EE} and $k_{EE} \neq 0$. The phase space of values of Equation S6 under these constraints is shown in Figure S2. Our results show that, similarly to the network with plastic $E \to E$ synapses (Figure 3), networks with both $E \to E$ and $E \to I$ plastic synapses can exhibit different types of non-linear contrast response. The type of nonlinearity (i.e sublinearity, supralinearity or supersaturation) is determined by the synaptic parameters w^o_{EE}, w^o_{IE}, k_{EE}, and k_{IE}.

Linear stability analysis

Our results show that plastic $E \to E$ synapses control the response to contrast in balanced networks δ. The contrast response function can be sublinear, supralinear or supersaturating depending on the synaptic parameters (Figure 2). Yet, the existence of these different steady states does not guarantee that they are stable in balanced networks. Here, we analyze the stability of the steady states in networks with plastic $E \to E$ synapses. Let us begin by assuming linear dynamics for $\nu_E(t)$ and $w^o_{EE}(t)$ in the vicinity of the steady state. The excitatory firing rate ν_E converges to the steady state ν^s_E with timescale τ_n. Similarly, the synaptic plasticity factor w^o_{EE} converges to the steady state value $w^o_{EE_s}$ with timescale τ_s. $w^o_{EE_s}(t)$ is determined by the network firing rate, such that $w^o_{EE_s}(t) = w^o_{EE_s}(\nu_E(t))$. In cortical networks, the excitatory and inhibitory currents have been shown to correlate with milisecond precision [7]. In line with these observations, we assume that the firing rates balance instantaneously such that $\tau_n \ll \tau_s$. This implies that (see Equation 14)

$$\nu_E(t) = \frac{c}{qp_E} \frac{J_{EI} - J_{II}}{J_{II}J_{EE}w^o_{EE}(t) - J_{EI}J_{IE}} \tag{S7}$$

holds at all times t. With this, we are left with one differential equation for the synapses in the vicinity of the fixed points

$$\tau_s \dot{w}^o_{EE}(t) = w^o_{EE_s}(\nu_E(t)) - w^o_{EE}(t) \tag{S8}$$

We compute $\frac{\partial \dot{w}^o_{EE}}{\partial w^o_{EE}}$ and evaluate it at the steady state $w^o_{EE_s}$. The sign of $\frac{\partial \dot{w}^o_{EE}}{\partial w^o_{EE}}$ indicates the stability of the steady state. If $\frac{\partial \dot{w}^o_{EE}}{\partial w^o_{EE}} < 0$, the steady state is stable as perturbations around the steady state are absorbed and the system is pushed back to the equilibrium point. If $\frac{\partial \dot{w}^o_{EE}}{\partial w^o_{EE}} > 0$, the steady state is unstable as perturbations around the steady state are amplified and the system is pushed away from the equilibrium point. From Equation S8, we obtain

$$\begin{aligned}
\tau_s \frac{\partial \dot{w}^o_{EE}}{\partial w^o_{EE}} &= \frac{\partial}{\partial w^o_{EE}}(w^o_{EE_s}(\nu_E) - w^o_{EE}) \\
&= \frac{\partial w^o_{EE_s}}{\partial \nu_E} \frac{\partial \nu_E}{\partial w^o_{EE}} - 1 \\
&= \left(\frac{\partial w^o_{EE_s}}{\partial \nu_E} \frac{c}{qp_E} \frac{J_{II}J_{EE}(J_{II} - J_{EI})}{(J_{II}J_{EE}w^o_{EE} - J_{EI}J_{IE})^2} - 1 \right)
\end{aligned} \tag{S9}$$

Next, we substitute c by using the balanced state expression (see Equation S7). This yields

$$\tau_s \frac{\partial \dot{w}^o_{EE}}{\partial w^o_{EE}} = -\left(\frac{\partial w^o_{EE_s}}{\partial \nu_E} \frac{\nu_E(J_{II}J_{EE})}{J_{II}J_{EE}w^o_{EE} - J_{EI}J_{IE}} + 1 \right) \tag{S10}$$

We now evaluate this expression for $w^o_{EE} = w^o_{EE_s}$ and make use of the definition of the synaptic efficacy k_{EE} introduced in the main text (Equation 4): here $\mathrm{k}_{EE} = \frac{\partial w^o_{EE_s}}{\partial \nu_E} \frac{\nu_E}{w^o_{EE}}$. We substitute k_{EE} into Equation S10, which yields

$$\begin{aligned}
\tau_s \frac{\partial \dot{w}^o_{EE}}{\partial w^o_{EE}} &= -\left(\frac{\mathrm{k}_{EE}w^o_{EE}(J_{II}J_{EE})}{J_{II}J_{EE}w^o_{EE} - J_{EI}J_{IE}} + 1 \right) \\
&= -\left(\frac{\mathrm{k}_{EE}w^o_{EE}}{w^o_{EE} - \frac{J_{EI}J_{IE}}{J_{II}J_{EE}}} + 1 \right).
\end{aligned} \tag{S11}$$

Using $\beta = \frac{J_{EI}J_{IE}}{J_{II}J_{EE}}$, the above expression transforms into

$$\begin{aligned}\tau_s \frac{\partial \dot{w}^o_{EE}}{\partial w^o_{EE}} &= -\left(\frac{w^o_{EE}(\mathrm{k}_{EE}+1)-\beta}{w^o_{EE}-\beta}\right) \\ &= -\frac{1}{\delta}\end{aligned} \tag{S12}$$

where δ is the susceptibility to input in balanced networks. From this, we conclude that the supersaturation regime ($\delta < 0$) is not stable in the limit of balanced networks. Both sublinear and supralinear regimes ($\delta > 0$) are stable.

Estimation of the firing rate ν in Model V

In a spiking network simulation, the firing rate is usually obtained *a posteriori*, by dividing the number of spikes that occurred over a given time frame. In the context of power-law synapses, the firing rate needs to be estimated for each neuron, upon firing, in order to determine the amplitude of the post-synaptic potential:

$$w^{ij}_{ab} = \left(\frac{\nu_{b,j}}{\nu_0}\right)^{\mathrm{k}}. \tag{S13}$$

Typically, the firing rate of each neuron is estimated by counting the number of spikes emitted in a given period of time. This approach has multiple drawbacks. First, the number of spikes emitted in a given time period is discrete, so the relative precision of the firing rate estimation decreases for low firing rates. Second, the synapses would display limited responsiveness, as they cannot adapt to new states faster than the time needed to renew the time window. Finally, the choice of the optimal length of the time window is a trade-off between a better precision (long period of time) and responsiveness (short period of time). Making this trade-off is especially difficult in networks with feature-dependent connectivity and input, in which neurons of the same population have a wide range of firing rates. Instead, we choose to estimate the firing rates using the n interspike intervals (ISIs) that precede any new spike. Assuming that the neuron's spiking follows a Poisson process and that the system is in steady state (all ISIs follow the same distribution), the sum of the n ISIs should follow an Erlang distribution

$$P_{\Sigma\mathrm{ISI}}(t) = \frac{\nu^n t^{n-1} e^{-\nu t}}{(n-1)!}, \tag{S14}$$

where ΣISI is the sum of n ISIs, and ν is the firing rate of the neurons. The mean of the n ISIs is given by

$$\langle ISI \rangle = \frac{\Sigma ISI}{n}. \tag{S15}$$

With the change of variable $\tau = \frac{t}{n}$

$$\begin{aligned}P_{\langle ISI \rangle}(\tau)d\tau &= P_{\Sigma ISI}(n\tau)n d\tau \\ &= \nu^n \tau^{n-1} e^{-\nu n \tau} \frac{n^n}{(n-1)!}.\end{aligned} \tag{S16}$$

Following the same approach, the pdf of the inverse of the average ISI ($\langle ISI \rangle^{-1}$) can be obtained with the change of variable $f = \frac{1}{\tau}$

$$\begin{aligned} P_{\langle ISI \rangle^{-1}}(f)df &= P_{\langle ISI \rangle}(f^{-1})\frac{-df}{f^2} \\ &= \frac{\nu^n}{f^{n+1}}\frac{n^n}{(n-1)!}e^{-\frac{n\nu}{f}}. \end{aligned} \tag{S17}$$

For $n > 1$, the expected value of $\langle ISI \rangle^{-1}$ is given by

$$\begin{aligned} E[\langle ISI \rangle^{-1}] &= \int_0^\infty f P_{\langle ISI \rangle^{-1}}(f)df \\ &= \frac{n^n}{(n-1)!}\int_0^\infty \frac{\nu^n}{f^n}e^{-\frac{n\nu}{f}}df. \end{aligned} \tag{S18}$$

With one last change of variable $g = \dfrac{n\nu}{f}$

$$\begin{aligned} E[\langle ISI \rangle^{-1}] &= -\frac{n^n}{(n-1)!}\int_\infty^0 \frac{\nu^n g^n}{n^n \nu^n}e^{-g}\frac{n\nu}{g^2}dg \\ &= \frac{\nu n}{(n-1)!}\int_0^\infty g^{n-2}e^{-g}dg \\ &= \frac{\nu n}{(n-1)!}\Gamma(n-1) \\ &= \frac{\nu n}{(n-1)!}(n-2)! \\ &= \frac{n}{n-1}\nu. \end{aligned} \tag{S19}$$

We can therefore build an estimator $\hat{\nu}$ of the neuron's firing rate based on the n ISIs that precede the time of evaluation:

$$\begin{aligned} \hat{\nu} &= \langle ISI \rangle^{-1}\frac{n-1}{n} = \frac{n-1}{\sum_{i=1}^n ISI_i} \\ E[\hat{\nu}] &= \nu. \end{aligned} \tag{S20}$$

Firing rate profile ν_E of balanced networks with feature-dependent connectivity

In this section, we outline a rate formalism of balanced networks with feature-dependent connectivity and plastic synaptic weights.

The firing rate of the presynaptic population $a = \{E, I\}$ is given by $\nu_a(\theta) \equiv [\langle s_{a,i}(t) \rangle]$, where $\theta = \frac{i}{N_a}$ and $s_{a,i}(t) = \delta(t - {t_n}^{a,i})$ is the spike train of the i-th neuron from population a, and ${t_n}^{a,j}$ are its spike times. In the continuum limit, the mean input currents are related to the firing rates as follows

$$\mu_a(\theta) \equiv \langle [I_i^a(\theta, t)] \rangle = \sqrt{N}\mu(\theta) + \int_{-\infty}^{\infty} \big(\lambda_E \frac{J_{aE}}{\sqrt{N}} p_{aE}(\theta - \psi)(w_{aE}^0 \nu_E)(\psi) - \lambda_I \frac{J_{aI}}{\sqrt{N}} p_{aI}(\theta - \psi)(w_{aI}^0 \nu_I)(\psi)\big)d\psi, \tag{S21}$$

where $\langle \cdot \rangle$ denotes temporal average, $[\cdot]$ denotes population average. The synaptic plasticity factor $w_{ab}^0(\nu_b(\theta))$ modulates the synaptic strength J_{ab} as a function of the presynaptic activity. The term $\mu(\theta)$ denotes a

feature-dependent external input, λ_b is the linear density of population b in the feature space. Since we assume the feature space Γ to have length 1, we have $\lambda_b = N_b$.

For $\mu_a(\theta)$ to be finite, the following condition must be met:

$$J_{aE}\frac{N_E}{N}p_{aE}(\theta) * (w^0_{aE}\nu_E)(\theta) - J_{aI}\frac{N_I}{N}p_{aI}(\theta) * (w^0_{aI}\nu_I)(\theta) + \mu(\theta) = \mathcal{O}\big(\frac{1}{\sqrt{N}}\big), \tag{S22}$$

where $*$ is the convolution in the feature space. Taking the limit $N \to \infty$ and writing the resulting equation in the Fourier domain we get

$$\begin{aligned} qJ_{EE}\widehat{p_{EE}}(\widehat{w^0_{EE}\nu_E}) - (1-q)J_{EI}\widehat{p_{EI}}(\widehat{w^0_{EI}\nu_I}) + \widehat{\mu} = 0 \\ qJ_{IE}\widehat{p_{IE}}(\widehat{w^0_{IE}\nu_E}) - (1-q)J_{II}\widehat{p_{II}}(\widehat{w^0_{II}\nu_I}) + \widehat{\mu} = 0, \end{aligned} \tag{S23}$$

where $q = \frac{N_E}{N}$ and $1-q = \frac{N_I}{N}$ are the fractions of excitatory and inhibitory neurons, respectively. Assuming the inhibitory connections are constant ($w^0_{EI} = w^0_{II}$=1), and setting p_{EE}=p_{IE}=p_E and p_{EI}=p_{II}=p_I the balanced state solution in the Fourier domain yields

$$J_{EE}J_{II}(\widehat{w^0_{EE}\nu_E}) - J_{EI}J_{IE}(\widehat{w^0_{IE}\nu_E}) = \frac{\widehat{\mu}}{\widehat{p_E}}\frac{J_{EI}-J_{II}}{q}. \tag{S24}$$

We set the feedforward input $\mu(\theta)$ to be a gaussian function of preferred feature:

$$\mu(\theta) = ce^{-\frac{(\theta-\theta_0)^2}{2\sigma^2_{stim}}}, \tag{S25}$$

where c is the stimulus contrast, σ^2_{stim} is the tuning width of the feedforward input and θ_0 is the input feature.

Neurons with a similar preferred feature are more likely to be connected. We assume it is given as a Gaussian function:

$$p_{ab}(\theta-\psi) = p_{max_b}e^{-\frac{(\theta-\psi)^2}{2\sigma^2_b}}, \tag{S26}$$

where p_{max_b} is the peak probability of connection, for two neurons sharing the same feature preference, θ and ψ are the feature preference of the postsynaptic and presynaptic neurons, and σ_b is the width of the distribution. The number of connections C_b from population b is given by

$$C_b = p_{max_b}\int_{-\infty}^{\infty} e^{-\frac{(\theta-\psi)^2}{2\sigma_b}}\lambda_b d\psi = \lambda_b\sigma_b\sqrt{2\pi}p_{max_b}. \tag{S27}$$

From this, we can define the connection probability with respect to the presynaptic population, such that $C_b = p_b N_b$:

$$p_b = p_{max_b}\sigma_b\sqrt{2\pi}. \tag{S28}$$

The excitatory firing rate profile can be expressed in the Fourier domain as

$$\frac{J_{EE}J_{II}(\widehat{w^0_{EE}\nu_E}) - J_{EI}J_{IE}(\widehat{w^0_{IE}\nu_E})}{J_{EI}-J_{II}} = c\frac{\sigma_{stim}\sqrt{2\pi}}{qp_E}e^{-if\theta_0}e^{-\frac{f^2(\sigma^2_{stim}-\sigma^2_E)}{2}}, \tag{S29}$$

and can be transformed back into the feature space:

$$\frac{J_{EE}J_{II}w^0_{EE}(\nu_E)\nu_E - J_{EI}J_{IE}w^0_{IE}(\nu_E)\nu_E}{J_{EI}-J_{II}} = c\frac{\sigma_{stim}}{qp_E\sqrt{\sigma^2_{stim}-\sigma^2_E}}e^{-\frac{(\theta-\theta_0)^2}{2(\sigma^2_{stim}-\sigma^2_E)}}. \tag{S30}$$

Note that networks of uniformly randomly connected neurons with orientation-dependent input ($\sigma_E \to \infty$) do not have a $\nu_E(\theta)$ solution in the balanced state. If the synaptic plasticity factor in $E \to E$ connections is the same as in $E \to I$ connections, the previous expression can be simplified as

$$w^0_{EE}(\nu_E)\nu_E = c\frac{J_{EI}-J_{II}}{J_{EE}J_{II}-J_{EI}J_{IE}}\frac{\sigma_{stim}}{qp_E\sqrt{\sigma^2_{stim}-\sigma^2_E}}e^{-\frac{(\theta-\theta_0)^2}{2(\sigma^2_{stim}-\sigma^2_E)}}. \tag{S31}$$

Finally, if the synaptic plasticity follows a power law, $w^0_{EE} = \left(\frac{\nu_E}{\nu_0}\right)^{\mathrm{k}}$, the firing rate response can be factorized into a function of contrast and a function of orientation:

$$\nu_E = \left(c\frac{J_{EI}-J_{II}}{J_{EE}J_{II}-J_{EI}J_{IE}}\frac{\sigma_{stim}\nu^{\mathrm{k}}_0}{qp_E\sqrt{\sigma^2_{stim}-\sigma^2_E}}\right)^{\frac{1}{\mathrm{k}+1}}e^{-\frac{(\theta-\theta_0)^2}{2(\mathrm{k}+1)(\sigma^2_{stim}-\sigma^2_E)}}. \tag{S32}$$

Supplementary tables and figures

Model I	
Populations	$N_E = [1.6 \times 10^4 ... 6 \times 10^4]$; $N_I = [4 \times 10^4 ... 1.5 \times 10^4]$ (neurons)
Connectivity	Random, $p_E = \bar{p_E} = 0.05$; $p_I = \bar{p_I}$=0.05
Synaptic weights	$J_{EE} = 2.5$; $J_{EI} = 10$; $J_{IE} = 4$; $J_{II} = 13.5$ (mV/spike)
Synaptic plasticity	No
Input	Orientation-independent, $c = [0...2.5]$ (mV/s)
Model II	
Populations	$N_E = 10^5$; $N_I = 2.5 \times 10^4$ (neurons)
Connectivity	Random, $p_E = \bar{p_E} = 0.05$, $p_I = \bar{p_I}$=0.05
Synaptic weights	$J_{EE} = 8$; $J_{EI} = 10$; $J_{IE} = 4$; $J_{II} = 13.5$ (mV/spike)
Synaptic plasticity	STP in $E \to E$: Facilitation: $U = 0.05$, $\tau_F = 0.8$ ms, $\tau_D = 0.03$ ms Depression: $U = 0.35$, $\tau_F = 0.15$ ms, $\tau_D = 0.7$ ms
Input	Orientation-independent, $c = [0...2.5]$ (mV/s)
Model III	
Populations	$N_E = 2 \times 10^5$; $N_I = 5 \times 10^4$ (neurons)
Connectivity	Orientation-dependent, $\bar{p_E} = \bar{p_I} = 0.05$; σ_E=σ_I=0.1
Synaptic weights	$J_{EE} = 2.5$; $J_{EI} = 10$; $J_{IE} = 4$; $J_{II} = 13.5$ (mV/spike)
Synaptic plasticity	No
Input	Tuned gaussian input, $c = 1, 2, 3$ (mV/s), $\sigma_{stim} = 0.16$
Model IV	
Populations	$N_E = 4 \times 10^5$; $N_I = 10^5$ (neurons)
Connectivity	Orientation-dependent, $\bar{p_E} = \bar{p_I} = 0.05$; σ_E=σ_I=0.1
Synaptic weights	$J_{EE} = 8$; $J_{EI} = 10$; $J_{IE} = 4$; $J_{II} = 13.5$ (mV/spike)
Synaptic plasticity	STP in $E \to E$: Facilitation: $U = 0.05$, $\tau_F = 0.8$ ms, $\tau_D = 0.03$ ms Depression: $U = 0.2$, $\tau_F = 0.2$ ms, $\tau_D = 0.2$ ms
Input	Tuned gaussian input, $c = [0...4]$ (mV/s), $\sigma_{stim} = 0.16$
Model V	
Populations	$N_E = 4 \times 10^5$; $N_I = 10^5$ (neurons)
Connectivity	Orientation-dependent, $\bar{p_E} = \bar{p_I} = 0.05$; σ_E=σ_I=0.1
Synaptic weights	$J_{EE} = 2$; $J_{EI} = 10$; $J_{IE} = 5$; $J_{II} = 12$ (mV/spike)
Synaptic plasticity	Power-law plasticity in $E \to E$ and $E \to I$: Synaptic efficacy k = -0.5
Input	Tuned gaussian input, $c = 0.5, 1, 1.5, 2$ (mV/s), $\sigma_{stim} = 0.16$
Model VI	
Populations	Figure 6: $N_{E_{dep}} = 3.2 \times 10^5$; $N_{E_{fac}} = 8 \times 10^4$ $N_I = 10^5$ (neurons) Figure S6: $N_E = 4 \times 10^5$; $N_I = 10^5$ (neurons)
Connectivity	Orientation-dependent, $\bar{p_E} = \bar{p_I} = 0.05$; σ_E=σ_I=0.1
Synaptic weights	$J_{EE} = 10$; $J_{EI} = 10$; $J_{IE} = 27$; $J_{II} = 13.5$ (mV/spike)
Synaptic plasticity	STP in $E \to E$ and $E \to I$: Figure 6: Facilitation: $U = 0.05$, $\tau_F = 0.8$ ms, $\tau_D = 0.03$; Depression: $U = 0.6$, $\tau_F = 0.3$ ms, $\tau_D = 1$ ms; $\alpha = 0.2$ Figure S6: Depression: $U = 0.2$ ms, $\tau_F = 0.2$ ms, $\tau_D = 0.2$ ms
Input	Tuned gaussian input, $\sigma_{stim} = 0.16$ Figure 6: $c = 0.5, 1, 1.5, 2$ (mV/s); Figure S6: $c = 0.5, 2, 3.5, 5$ (mV/s)

Table S1: Parameters for each network model. For all spiking network models: $\tau_m = 20$ (ms), $V_{th} = 1$ (mV), $v_{rest} = 0$ (mV), $\sigma_\theta = 2$ mV/$\sqrt{s}$, the simulation time step $dt = 0.05$ (ms), and the recording bin size is 50 ms. The synaptic weights and the input are re-scaled by $\frac{1}{\sqrt{N}}$ and $\sqrt{N}$, respectively (see Equation 8) [8]. Let us note that we re-scale the feature space Γ, σ_E and σ_I to 180° in the figures for illustration purposes.

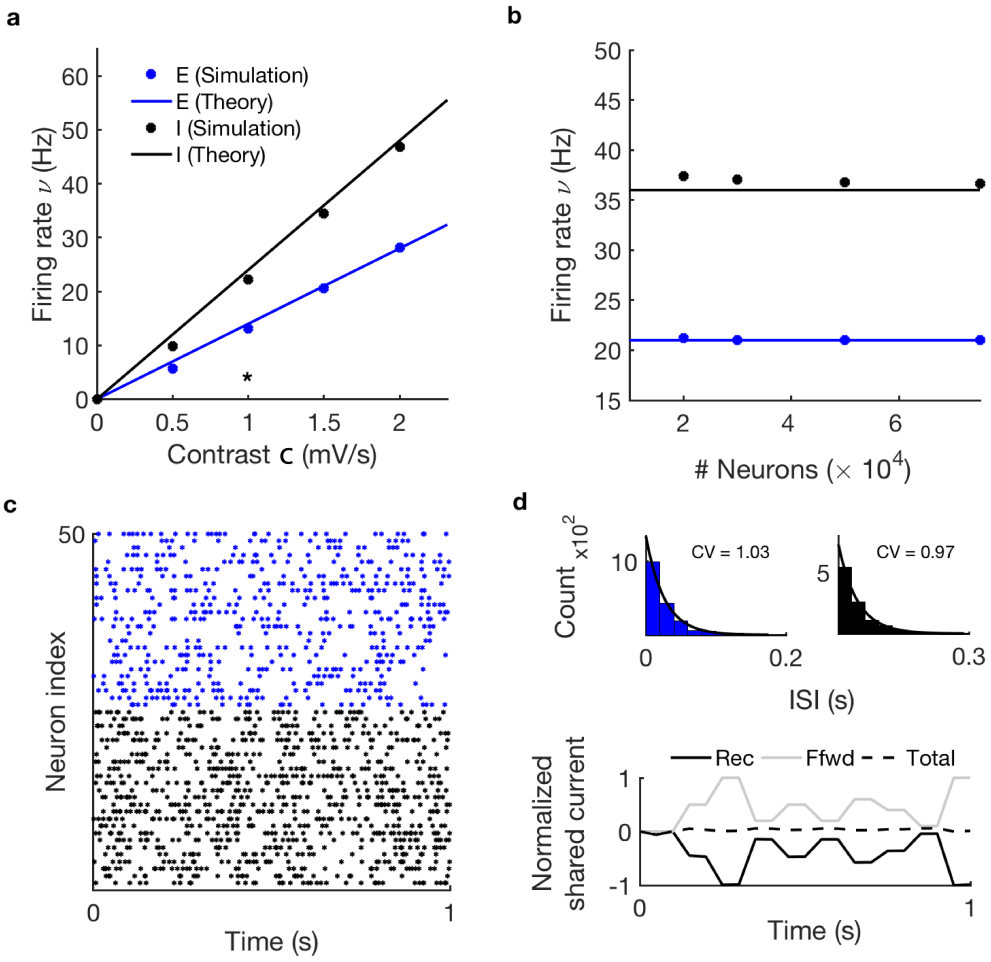

Figure S1: **Linear response to contrast for uniform networks of randomly connected LIF neurons and constant synapses. (a)** The mean activity of the excitatory (blue) and the inhibitory (black) populations in a network of $N = 5 \cdot 10^4$ LIF neurons (dots) with constant synapses ($w^o_{ab} = 1$) is captured by the balanced state equations (Equation 10, solid lines). **(b)** An increase in the number of neurons from $N = 2 \cdot 10^4$ to $N = 5 \cdot 10^4$ corrects a maximum deviation from balance (solid lines) of 4.5%. **(c)** Spike raster of 25 excitatory and 25 inhibitory neurons across 1 s for the data point denoted by an asterisk in (a). **(d)** Top: coefficient of variation (CV), inter-spike interval (ISI) distribution and exponential fit for the data point denoted by asterisk in (a) indicate asynchronous irregular firing. Bottom: temporal correlations of the E and I inputs estimated for data point denoted by asterisk in (a) indicate E-I balance. For parameters see Table S1, Methods – Model I.

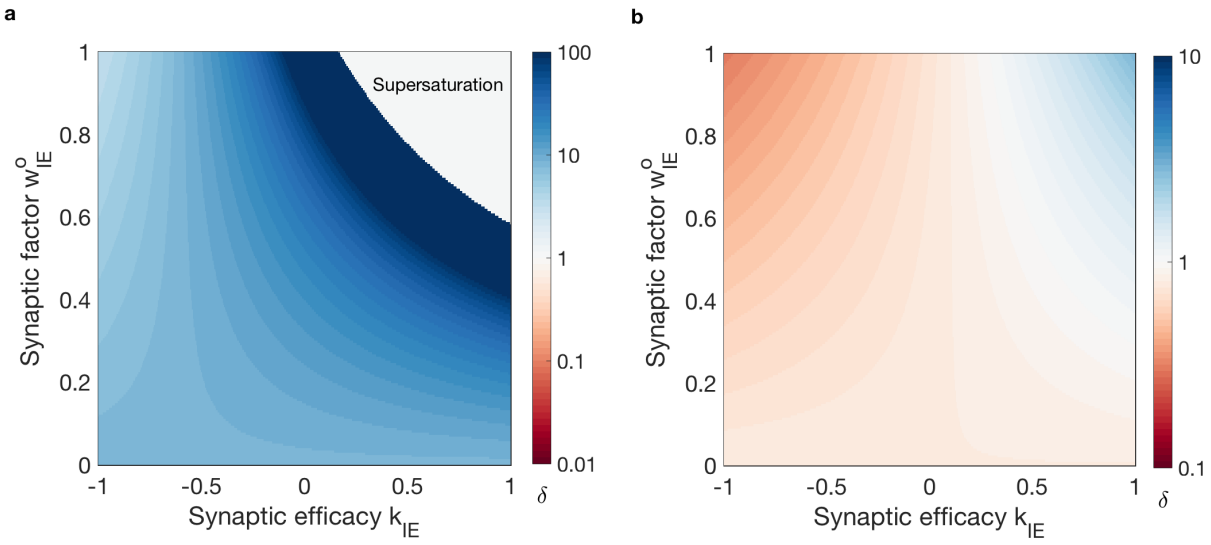

Figure S2: **Susceptibility to contrast δ in networks with plastic $E \to E$ and $E \to I$ synapses. (a)** The phase space of values for δ (Equation S6) for $w^o_{EE} = 0.4$ and $k_{EE} = -0.6$ (depressing state). **(b)** The phase space of values for δ (Equation S6) for $w^o_{EE} = 0.4$ and $k_{EE} = 0.1$ (facilitating state). Let us note that for positive input contrast and $J_{II} > J_{EI}$, parameters must satisfy $w^o_{IE} < \frac{w^o_{EE}}{\beta}$ for positive firing rates [8, 9].

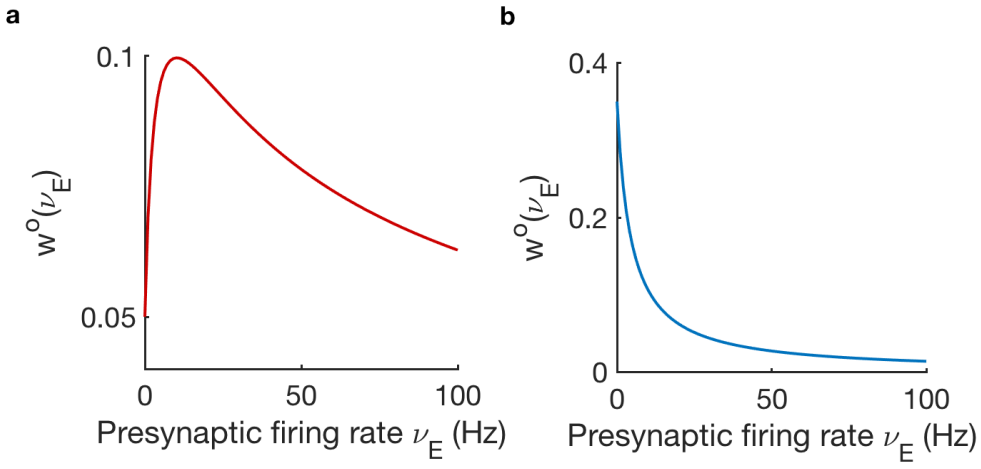

Figure S3: **Steady-state probability of neurotransmitter release $w^o(\nu_E)$ (Equation S3). (a)** Facilitating transmission: w^o increases until neurotransmitter vesicles can not replenish fast enough to be released upon spike arrival. At this point, w^o decreases for increasing ν_E. Parameters: $U = 0.05$, $\tau_F = 0.8$ ms, $\tau_D = 0.3$ ms. This function models the $E \to E$ synapses in Figures 2, 3, 4, and 6. **(b)** Depressing transmission: w^o decreases with increasing ν_E as a result of neurotransmitter not being available. Parameters: $U = 0.35$, $\tau_F = 0.15$ ms, $\tau_D = 0.7$ ms. This function models the $E \to E$ synapses in Figures 2 and 3.

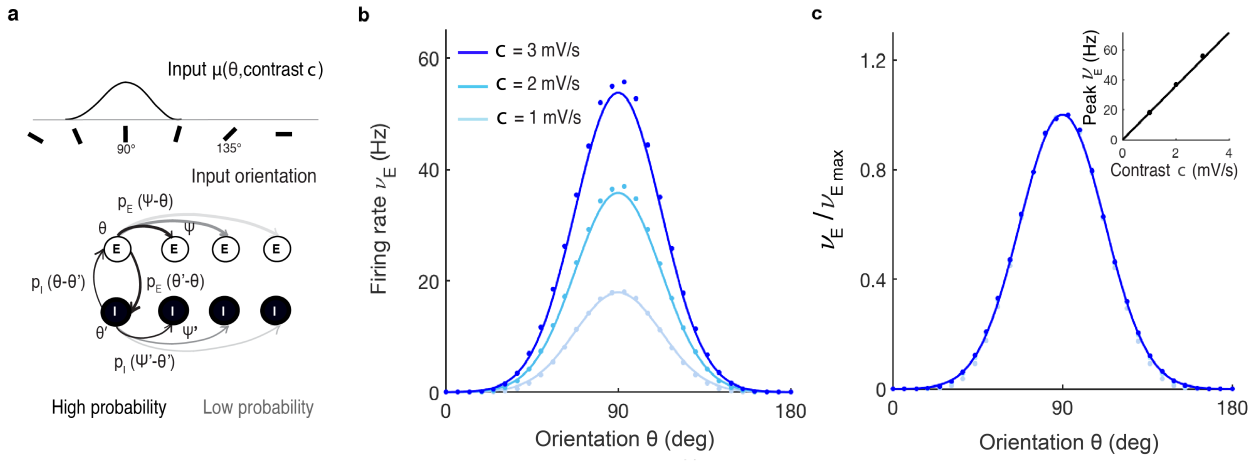

Figure S4: **Networks with orientation-dependent connectivity and constant synapses have linear susceptibility and are contrast-invariant. (a)** A Network with feature-dependent connectivity (see Methods - Model III and Table S1 for parameters). The connection probability functions p_E and p_I are Gaussian. **(b)** Excitatory tuning curves in response to different input contrast, $c = 1, 2, 3$ (mV/s). Prediction from the balanced theory (Equation 10, solid lines) compared to the results obtained in a simulation of spiking neurons (dots). **(c)** Overlapping normalized tuning curves from (b) show contrast invariance. Inset: peak firing rate at $\theta = 90°$ from tuning curves in (b) linearly increases with contrast.

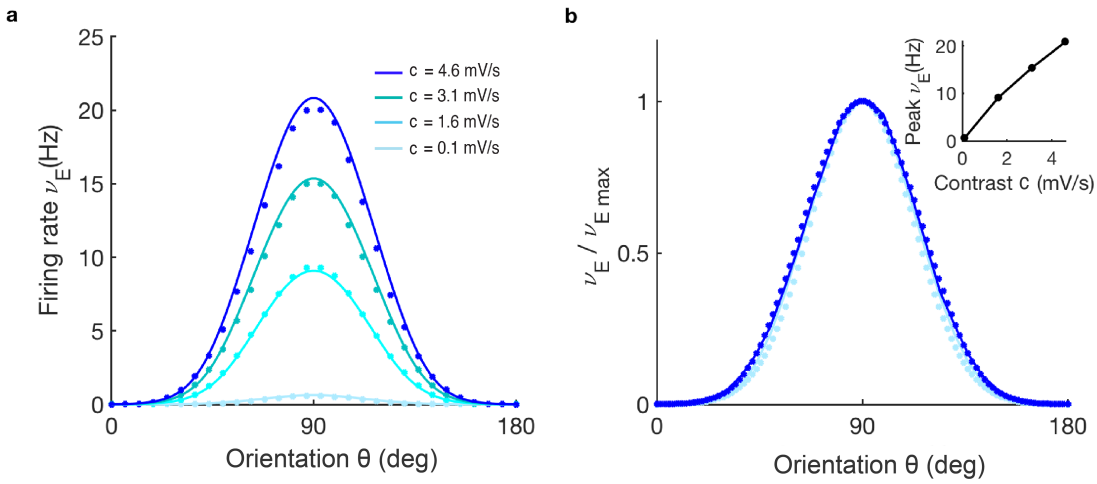

Figure S5: **Depressing $E \to E$ STP induces sublinear susceptibility to contrast and leads to quasi-invariant network selectivity.** Same network model as in Figure 4a with depressing $E \to E$ STP synapses (see Methods - Model IV and Table S1). **(a)** Excitatory tuning curves for different input contrast, $c = 0.1, 1.6, 3.1, 4.6$ (mV/s), in a mean-field network description (Equation 5, solid lines) compared to spiking network simulations of $N = 5{\cdot}10^5$ neurons (dots). Notice the difference in tuning curves compared to a network with facilitating STP $E \to E$ synapses (Figure 4b). **(b)** Normalized excitatory tuning curves in (a) show a quasi-invariant selectivity as a function of input contrast. Inset: firing rate of tuning curves in (a) in spiking networks (dots) and balanced theory (solid line) for $\theta = 90°$.

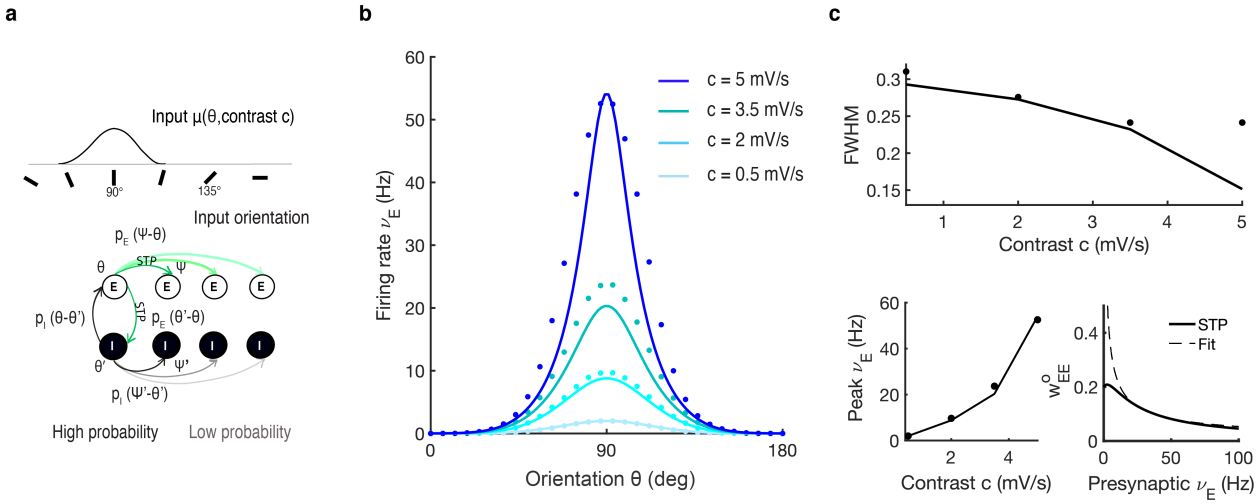

Figure S6: **Depressing STP in the $E \to E$ and $E \to I$ synapses induces a supralinear response to contrast and narrows the network selectivity.** **(a)** Network with orientation-dependent connectivity. Plastic synapses (green) follow depressing STP dynamics (see Methods - Model VI and Table S1). **(b)** Excitatory tuning curves for different input contrast, $c = 0.5, 2, 3.5, 5$ (mV/s), in a mean-field network description (Equation 10, solid lines) compared to spiking network simulations of $N = 5 \cdot 10^5$ neurons (dots). **(c)** Top: full width at half maximum (FWHM) for the contrasts c analyzed in b. The difference between spiking and mean-field data for $c = 5$ mV/s could be due to variations between the STP firing rate approximation to the synaptic spiking model for those firing rates (Equation S3). Bottom left: firing rate at the preferred orientation ($\theta = 90°$) as a function of contrast. Bottom right: average neurotransmitter release probability, $\mathrm{w}^o_{\mathrm{EE}}$ as a function of contrast and fit to a power-law for $\nu_E > 10$ Hz (dashed line).

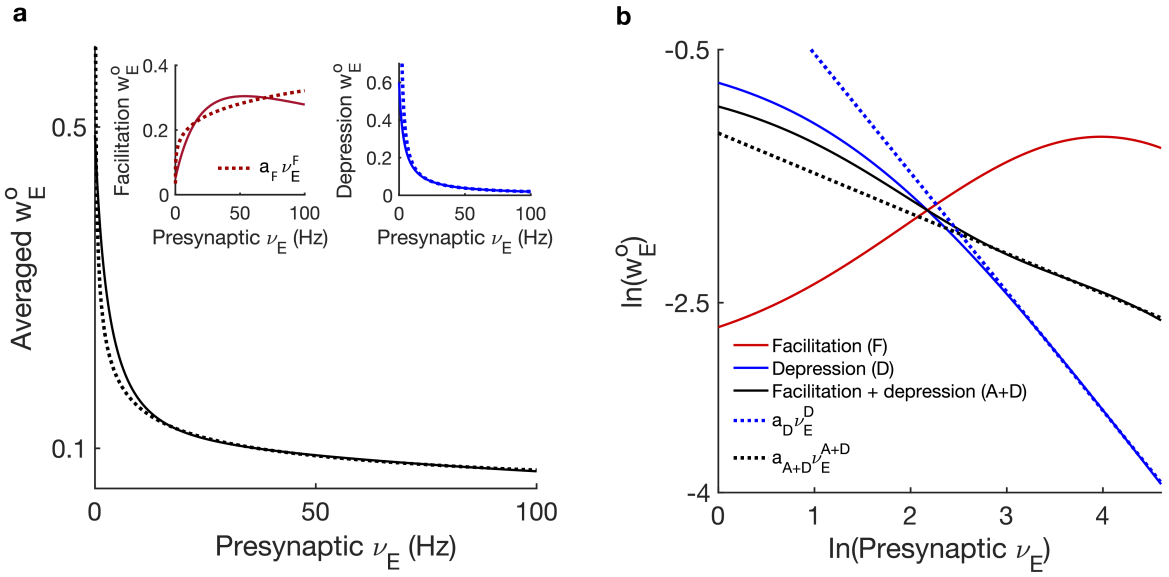

Figure S7: **STP synaptic transformation and approximation to a power-law. (a)** The effective probability of neurotransmitter release w^o_E in: a population of facilitating and depressing STP synapses (main plot, solid black, $\alpha = 0.2$, see Figure 6), facilitating STP synapses (inset, solid red), and depressing STP synapses (inset, solid blue) as a function of presynaptic firing rate ν_E. Dotted lines show the fit to a power-law for depression (blue), facilitation (red) and the combination of facilitation and depression (black). **(b)** Same as in (a) for logarithmic axis. The plot shows how the combination of facilitation and depression approximates a power-law better for low firing rate values compared to pure depression. Color code as in (a). Parameters as in Figure 6 - see Table S1.

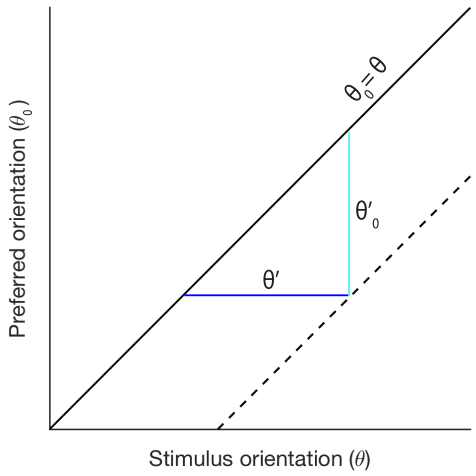

Figure S8: **The network response depends on the difference between the neuron's preference and the stimulus orientation.** Previous approaches have defined the network response to orientation ν as the mean activity of single neurons aligned at the preferred orientation [10]. This can be mathematically formalized as $\nu = \frac{1}{N}\sum_{\theta_0} f(\theta_0, \theta_0 + \theta')$. We have assumed a preferred orientation for each neuron and defined the network response as the mean activity of the neurons relative to the stimulus orientation. Mathematically, this implies that $\nu = \frac{1}{N}\sum_{\theta} f(\theta - \theta'_0, \theta)$. Here we show that both descriptions of the network response are equivalent as $\theta = \theta_0 + \theta'$.

.

Video S1: **Approximation for excitatory firing rate ν_E in a network with $E \to E$ plasticity with feature-dependent input** μ. Here, $\nu_E = \mu^{\delta(\mu)}$ is used, where for simplicity dimensionless quantities are used, and where we have used $\delta(\mu)$ as a first order approximation for $\delta(\nu_E)$. This is a valid approximation for δ close to unity. Here, $\mu = ce^{-\theta^2}$ and preferred orientation $\theta = 0$. As a plasticity rule, an STP-like rule $w(\nu) = (1 - e^{-\nu})e^{-0.3\nu}$ is used, where the term $(1 - e^{-\nu})$ implements facilitation and the subsequent term $e^{-0.3\nu}$ implements depression. Equation 1 is then used to derive the expression for $\delta(\nu)$. One can observe a regime for small contrasts $c < 1$ in which $\delta > 1$ in the preferred orientation, and in which ν_E narrows. This is followed by a regime $c > 1$ in which δ in the preferred orientation drops below unity, and the output firing rate broadens.

References

[1] Alex M Thomson and Jim Deuchars. Temporal and spatial properties of local circuits in neocortex. *Trends in neurosciences*, 17(3):119–126, 1994.

[2] Misha V Tsodyks and Henry Markram. The neural code between neocortical pyramidal neurons depends on neurotransmitter release probability. *Proceedings of the national academy of sciences*, 94(2):719–723, 1997.

[3] Juan A Varela, Kamal Sen, Jay Gibson, Joshua Fost, LF Abbott, and Sacha B Nelson. A quantitative description of short-term plasticity at excitatory synapses in layer 2/3 of rat primary visual cortex. *Journal of Neuroscience*, 17(20):7926–7940, 1997.

[4] Chris M Hempel, Kenichi H Hartman, X-J Wang, Gina G Turrigiano, and Sacha B Nelson. Multiple forms of short-term plasticity at excitatory synapses in rat medial prefrontal cortex. *Journal of neurophysiology*, 83(5):3031–3041, 2000.

[5] Gianluigi Mongillo, David Hansel, and Carl Van Vreeswijk. Bistability and spatiotemporal irregularity in neuronal networks with nonlinear synaptic transmission. *Physical review letters*, 108(15):158101, 2012.

[6] Lubomir Kostal, Petr Lansky, and Michael Stiber. Statistics of inverse interspike intervals: The instantaneous firing rate revisited. *Chaos: An Interdisciplinary Journal of Nonlinear Science*, 28(10):106305, 2018.

[7] Michael Okun and Ilan Lampl. Instantaneous correlation of excitation and inhibition during ongoing and sensory-evoked activities. *Nature neuroscience*, 11(5):535, 2008.

[8] Carl Van Vreeswijk and Haim Sompolinsky. Chaos in neuronal networks with balanced excitatory and inhibitory activity. *Science*, 274(5293):1724–1726, 1996.

[9] Robert Rosenbaum and Brent Doiron. Balanced networks of spiking neurons with spatially dependent recurrent connections. *Physical Review X*, 4(2):021039, 2014.

[10] Laura Busse, Alex R Wade, and Matteo Carandini. Representation of concurrent stimuli by population activity in visual cortex. *Neuron*, 64(6):931–942, 2009.